Title: Thioredoxin interacting protein (Txnip) forms redox sensitive high molecular weight nucleoprotein complexes

Short title: Txnip forms redox sensitive high molecular weight nucleoprotein complexes

Cristiane Lumi Hirata[1, 2], Shinji Ito[3], Hiroshi Masutani*[1,2]

[1]Tenri Health Care University, Tenri, 80-1 Bessho-cho, Tenri, Nara, 632-0018, Japan

[2]Department of Infection and Prevention, Institute for Frontier and Medical Sciences, Kyoto University, 53, Kawahara-cho, Shogoin, Sakyo, Kyoto, 606-8507, Japan

[3]Medical Research Center, Graduate School of Medicine, Kyoto University, Yoshida-Konoe-cho, Sakyo, Kyoto, 606-8501, Japan

Corresponding author:

*h.masutani@tenriyorozu-u.ac.jp

Abstract

Thioredoxin interacting protein (Txnip) is an α-arrestin protein that regulates pleiotropic biological responses. Txnip acts as a cancer suppressor and is a critical regulator of energy metabolism. To investigate molecular mechanisms involving Txnip, we searched for its protein binding partners using tandem affinity purification and proteomics analyses and identified several viable candidates, including HSP90, HSP70, and Prp31. We showed, by native PAGE, that Txnip is involved in the formation of high molecular weight complexes (1000 to 1300 kDa) in the nuclear fraction of cells treated with glucose and bortezomib. DTT treatment partly dissolved these high molecular weight complexes, suggesting that Txnip forms redox sensitive high-order nucleoprotein complexes. RNAse treatment slightly decreased the complex and RNA-seq showed differential expression of RNAs in the complex between Txnip protein overexpressing and control cells, indicating the involvement of RNAs in the complex. These results collectively provide a model whereby Txnip exerts its functions through multiple binding partners, forming transient higher-order complexes to regulate other signaling molecules.

Keywords: Txnip, α-arrestin, high molecular complex, redox, RNA, lncRNA

Introduction

Our group previously identified thioredoxin binding protein-2 (TBP-2) (1), which is also referred to as thioredoxin interacting protein (Txnip) (2). Txnip is an α-arrestin protein consisting of arrestin domains and conserved C-terminal PPxY motifs. It is reported to play important roles in a variety of cellular processes, including tumor suppression, regulation of inflammation, redox reactions, and metabolism. Considering its sequence homology to β-arrestins, it is assumed that Txnip acts through protein-protein interactions. However, Txnip binding partners have not been elucidated.

Suberoylanilide hydroxamic acid (SAHA; Vorinostat), a histone deacetylase (HDAC) inhibitor, induces Txnip expression (3). As for subcellular localization, Txnip accumulates in the nucleus after treatment with SAHA (4).

Under high glucose conditions, carbohydrate-responsive element-binding protein (chREBP)/max-like protein (Mlx), and Mlx-interacting protein (MondoA)/Mlx mediate upregulation of Txnip (5). In addition to transcriptional activation of the *Txnip* gene, glucose augments Txnip expression by inhibiting AMP-

dependent kinase (AMPK), which is a key regulator of energy homeostasis (6,7). Moreover, Txnip is rapidly degraded by cellular proteasomal mechanisms (7). Although this process is thought to occur through the binding of Txnip PPxY motifs to the WW domains of the NEDD family of E3 ubiquitin ligases, such as Itch (8), the mechanisms regulating Txnip expression are not clarified yet. Various studies have shown that Txnip regulates glucose metabolism (9–12). Some reports have unveiled that Txnip represses glucose uptake, as observed in hepatic (5), adipose, and muscle cells (10). As Txnip deficiency augments insulin signaling and sensitivity, Txnip is implicated in the pathophysiology of diabetes (11,13). Nonetheless, the molecular mechanisms involving Txnip-mediated regulation of metabolism are still unknown.

Underlining its importance in human pathology, Txnip expression is downregulated in high-grade malignant cancer tissues (14–18). Lack of the *Txnip* gene augments hepatocarcinogenesis (16) and bladder cancer (18) in mice. In a previous study, we showed that deficiency in Txnip enhances TGF-β signaling and promotes epithelial to mesenchymal transition (EMT) (19). However, the mechanisms of tumor suppression by Txnip are not completely elucidated.

Txnip is reported to interact with various molecules, such as thioredoxin (TRX) (1,20) (inhibiting its reducing and antioxidant activities), JAB1 (21), NLRP3 (22), and protein disulfide isomerases (PDIs) (23). However, these interactions cannot explain the wide variety of functions of Txnip.

In this work, we examined Txnip-interacting partners to investigate the molecular mechanisms of this multifunctional protein. Our results indicate that Txnip forms redox sensitive high molecular weight complexes with multiple binding partners found in the nucleus.

Materials and methods

Yeast two-hybrid assay

The Matchmaker GAL4 Two-Hybrid System 3 from Clontech (Mountain View, CA, USA) was used to perform the yeast two-hybrid assay according to the manufacturer's protocol. The pGBHKT7-Txnip vector, lacking the thioredoxin binding region, was introduced into yeast strain AH109 and selected colonies were expanded and transformed with a Jurkat cDNA library (Clontech). From the 360 yeast colonies growing on medium deficient in leucine, adenine, histidine, and tryptophan, genes from 16 colonies presenting β-

galactosidase activity were selected and sequenced. Genes from 9 clones had protein coding sequence in frame.

Cell culture

MCF7 (ATCC HTB-22) and HEK 293 (ATCC CRL-1573) cells were obtained from ATCC (Manassas, VA, USA), and were cultivated in Dulbecco's Modified Eagles Medium (DMEM) (D6046, Sigma-Aldrich, St. Louis, MO, USA) supplemented with 10% fetal bovine serum and 5% penicillin/streptomycin and incubated at 37°C under a 5% CO_2 atmosphere.

Transfection

The pCMV-Tag2A-Txnip vector was constructed as previously described (4) using pCMV-Tag2A vector obtained from Stratagene (La Jolla, CA, USA). From this pCMV-Tag2A-Txnip vector, we constructed pCMV-HA-Flag-Txnip by inserting Flag-Txnip into the pCMV-HA vector. pCMV-Tag3-Txnip was constructed using pCMV-Tag2A-Txnip vector. pTRE2pur-F-HA-Txnip-V5-His was constructed by inserting the site of NheI-PmeI of the pCMV-Flag-HA-Txnip vector into the NheI-EcoRV site of the pTRE2pur vector. pFN21A-Prp31-Halotag was bought from Promega (Madison, WI, USA) and the Prp31 gene sequence was amplified by PCR with primers 5′-GGATCCATGTCTCTGGCAGATGAGCTCTTA-3′ and 5′-CCGCGGTCAGGTGGACATAAGGCCACTCTT-3′, containing BamHI and SacII cloning sites. The amplified sequence was inserted into pCR-Blunt II-TOPO® (Invitrogen, Carlsbad, CA, USA) and then the BamHI-EcoRI cloning site was inserted into pCMV-Tag3B, resulting in pCMV-Tag3B-Prp31 vector. Vectors were transfected into cells with TransIT® reagent (Mirus Bio, Madison, WI, USA).

Antibodies and Reagents

Rabbit polyclonal *a*nti-VDUP1 (40-3700, Invitrogen) or rabbit monoclonal anti-Txnip (ab18865, Abcam) (referred here as anti-Txnip (Invitrogen) and anti-Txnip (Abcam), respectively), mouse monoclonal anti-HSP90αβ (StressMarq, SMC-135C/D, Victoria, BC, Canada), mouse monoclonal anti-HSP70 (Thermo Scientific, MA3-006, Waltham, MA, USA), and rabbit monoclonal anti-Prp31 (Abcam, ab188577) were used in this study. Immunoprecipitation beads used were anti-Flag®M2 Magnetic beads (Sigma-Aldrich), anti-HA magnetic beads (MBL, MA M132-11, Nagoya, Japan), anti-myc magnetic beads (MBL, M07-10, Nagoya, Japan) and Dynabeeds M-280 anti-mouse IgG (Invitrogen). The reagents used were glucose, DTT and Triton X-100 bought from Nacalai Tesque, Japan, SAHA (Enzo Life Sciences, Farmingdale, NY, USA), RNaseA

(Promega), Bortezomib (LC Laboratories, 179324-69-7, Woburn, MA), and MG132 (EMD Millipore, Burlington, MA, USA).

Immunoprecipitation and immunoblot Analysis

Protein extraction was performed using a hypotonic buffer (10 mM Hepes-KOH pH 7.9, 1.5 mM $MgCl_2$, 10 mM KCl, 0.5 mM DTT, protease inhibitor EDTA free (Nacalai Tesque)) for cytoplasmic protein fractions, and hypertonic buffer (20 mM Hepes-KOH pH 7.9, 1.5 mM $MgCl_2$, 420 mM NaCl, 0.5 mM DTT, 25% glycerol, protease inhibitor EDTA free (Nacalai Tesque)) for nuclear protein fractions. After nuclear protein extracts were transferred to another tube, the remaining pellet was dissolved in Triton X-100 lysis buffer (20 mM Tris-HCl pH 7.5, 150 mM NaCl, 1% Triton X-100, protease inhibitor EDTA free (Nacalai Tesque)) for extraction of less soluble nucleoprotein extracts. Total extracts were prepared using the Triton X-100 lysis buffer.

Affinity purification of the samples was performed as follows. Equal amounts of extracts from MCF7 cells expressing Flag-HA (control) and those expressing Flag-HA-Txnip were incubated with anti-Flag magnetic beads overnight at 4 °C. Beads were washed three times with 0.05 % Tween-PBS and then eluted with 3x Flag peptide (St. Louis, MO, USA). Eluates were then incubated with anti-HA magnetic beads overnight at 4 °C. Beads were washed three times with 0.05 % Tween PBS and then eluted with HA peptide. Extracts from 293 Tet-on cells stably transfected with either control vector or F-HA-Txnip-V5-His vector were incubated with anti-Flag magnetic beads overnight at 4 °C. Beads were washed three times with 0.05% Tween-PBS and then eluted with 3x Flag peptide (Sigma).

Extracts from MCF-7-F-HA-Txnip cells were incubated with anti-Myc magnetic beads or anti-Flag magnetic beads overnight at 4 °C. Beads were washed three times with 0.05 % Tween-PBS and eluted with 3x Flag peptide (Sigma). We performed immunoblotting as described previously (19). Images were captured using either GE ImageQuant LAS 4000 or Biorad ChemiDoc XRS.

Blue native PAGE

NativePAGE™ Novex® Bis-Tris 3-12% gel (1.0 mm x 10 wells) and respective buffers from Invitrogen were used. Samples were loaded with Tricine Sample Buffer (BioRad, Hercules, CA, USA) and electrophoresed at a constant 150 V in Dark Blue Cathode Buffer. After 30 min, the top portion of the running buffer was changed to Light Blue Cathode Buffer and electrophoresis was continued an additional 90 min. The gel was released from the plastic cast and incubated in SDS running buffer for 10 min. Proteins were

then transferred from the gel to a PVDF membrane was performed. Following transfer, the membrane was washed in 8% acetic acid for 15 min and washed in distilled water twice. Next, the membrane was soaked in methanol, washed with distilled water again, blocked with 5% skim milk-PBS-Tween solution, washed again and incubated with antibody overnight.

Mass Spectrometry Analysis

Affinity purified samples from less soluble nucleoprotein extracts were applied on a Precast Gel (MULTIGEL II mini 4/20 (13 W), Cosmo Bio, DCB-414879, Tokyo, Japan) and silver stained (Silver Stain for Mass Spectrometry, Prod. 24600, Pierce, Waltham, MA, USA). The silver-stained bands were excised, destained and digested in-gel with trypsin using the In-Gel Tryptic Digestion Kit (Thermo Fisher Scientific, Waltham, MA, USA) according to manufacturer's instructions. The protein digests were resuspended in 0.1% formic acid and separated using Nano-LC-Ultra 2D-plus equipped with cHiPLC Nanoflex (Eksigent, Dublin, CA, USA) in trap-and-elute mode, with a trap column (200 µm x 0.5 mm ChromXP C18-CL 3 µm 120 Å (Eksigent)) and an analytical column (75 µm x 15 cm ChromXP C18-CL 3 µm 120 Å (Eksigent)). Sample separation (described in Tables 2 and 3) was carried out using a binary gradient as follows: 2-40 % B for 50 min, 40-90 % B in 1 min, 90% B for 5 min, 90-2 % B in 0.1 min, and 2 % B for 18.9 min, where solvents A and B correspond to 0.1 % formic acid/2% acetonitrile/water and 0.1% formic acid/20% water/80% acetonitrile, respectively. For the samples in Table 4, the binary gradient used was as follows: 2-33.2 % B for 50 min, 33.2-98 % B in 2 min, 98 % B for 5 min, 98-2 % B in 0.1 min, and 2 % B for 17.9 min, where solvents A and B corresponds to 0.1% formic acid/water and 0.1 % formic acid/acetonitrile, respectively. The eluates were infused on-line to a mass spectrometer (TripleTOF 5600+ System with NanoSpray III source and heated interface (SCIEX, Framingham, MA, USA)) and ionized in an electrospray ionization-positive mode. Data acquisition was carried out using an information-dependent acquisition method. The acquired datasets were analyzed by ProteinPilot software version 4.5 beta (SCIEX) with the UniProtKB/Swiss-Prot database for humans (April 2013 for samples in Tables 2 and 3 and June 2016 for samples in Table 4) appended with known common contaminants (SCIEX). The quality of the database search was confirmed by the false discovery rate analysis in which the reversed amino acid sequences were used as a decoy. The reliability of protein identification was evaluated based on the numbers of peptides identified with a confidence of at least 95 %, and Unused ProtScores that were calculated by the Pro Group algorithm (SCIEX). The results were further evaluated by the comparison with parallel controls (size- and molecular weight-matched gel pieces were excised from the control lanes and processed simultaneously) and analysis of molecular weight information.

Results

Identification of potential candidate proteins binding with Txnip by yeast two-hybrid assay

We started our study with an artificial yeast two-hybrid assay. We used a pGBKT7-Txnip vector, without the thioredoxin binding region, as bait, to obtain Txnip-binding candidates other than thioredoxin. From 360 yeast colonies, 16 were selected, and from these, 9 genes were identified. The identified candidates are listed in Table 1.

Table 1. Identification of potential Txnip binding candidates by yeast two-hybrid assay using Txnip (lacking thioredoxin binding region) as bait

Gene	Location	Name
UXT	Nuclear	ubiquitously expressed transcript
SIVA1	Cytosol	SIVA1 apoptosis inducing factor
CBX8	Nuclear	chromobox homolog 8
IDI1	Cytosol	isopentenyl-diphosphate delta isomerase 1
EEF1A1	Cytosol	eukaryotic translation elongation factor 1 alpha 1
RUVBL2	Nuclear	RuvB-like 2
INTS9	Nuclear	integrator complex subunit 9
CROP	Speckled	cisplatin resistance-associated overexpressed protein
GAPDH	Cytosol	glyceraldehyde-3-phosphate dehydrogenase

Identification of Txnip binding partners by tandem purification, proteomic analysis, and mass spectrometry

To identify proteins bound to Txnip, we employed MCF7 breast cancer cells stably transfected with the pCMV-Flag-HA vector containing a Txnip sequence (MCF7-Flag-HA-Txnip). The cells were treated with SAHA and MG132, a proteasome inhibitor, to identify binding molecules that are relevant to the function and

accumulation of Txnip. SAHA was used to increase nuclear expression of Txnip (3, 4). Txnip has been shown to have an elevated turn over rate due to rapid degradation (7, 8), therefore we used the MG132 proteasome inhibitor. We extracted proteins from the less soluble nuclear fraction and pulled-down Txnip binding proteins once with anti-Flag or twice, in tandem, with anti-Flag and anti-HA. Eluted samples were separated on SDS-PAGE denaturing gels, which were then silver stained (Figure 1). Prominent bands were excised and analyzed by mass spectrometry (see Materials and methods for details). Candidate proteins, such as Hornerin and RuvB-like 1 were identified (Table 2, Supplementary Table 1).

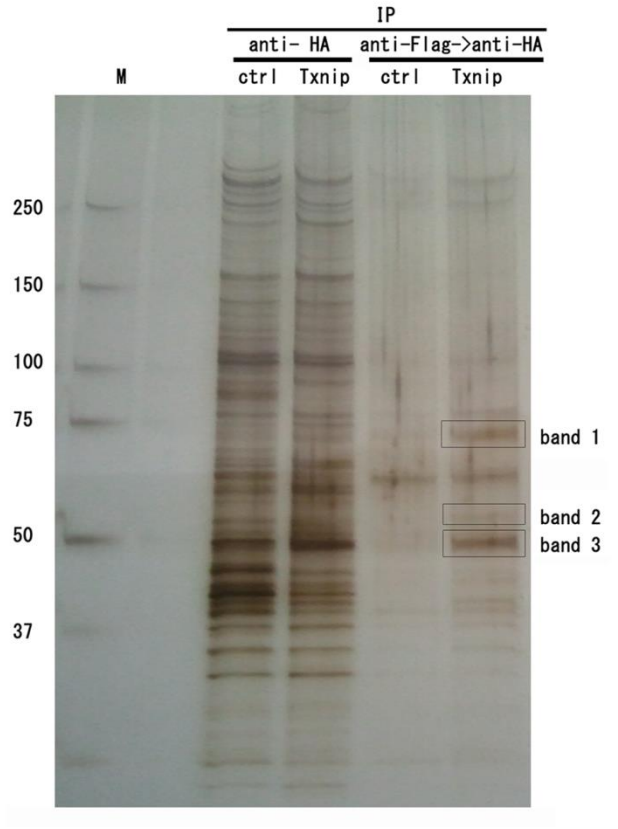

Figure 1. Identification of candidate proteins interacting with Txnip in MCF7 cells stimulated with SAHA and MG132. Silver staining of bands tandemly immunoprecipitated from extracts of MCF7-Flag-HA-Txnip (Txnip) or MCF7-Flag-HA (control). Extracts were prepared from cells stimulated with 2 μM SAHA and 2 μM MG132 for 6h and retrieved by Triton X-100 lysis buffer after discarding the cytosolic fraction. Equal amounts of extract from MCF7 cells expressing MCF7-Flag-HA (control) and those expressing MCF7-Flag-HA-Txnip were incubated with anti-HA or anti-Flag magnetic beads overnight at 4 °C. Beads were washed three times with 0.05 % Tween PBS and then eluted with HA peptide or 3x Flag peptide (Sigma), respectively. The Flag eluates were then incubated with anti-HA magnetic beads overnight at 4 °C. Beads were washed

three times with 0.05 % Tween PBS and then eluted using the HA peptide. The eluates were applied on a Precast Gel and silver stained. Indicated bands were analyzed by mass spectrometry. The image shown is a representative result of two repeated experiments. Candidate proteins are shown in Table 2 and Supplementary Table 1.

Table 2. Mass spectrometry results for candidate proteins interacting with Txnip in MCF7 cells stimulated with SAHA and MG132

Band	Name	ProtScore (Unused)	Matched peptides (95%)
1	Hornerin	2	1
	Lymphoid-restricted membrane protein	2	1
	Ubiquitin-60S ribossomal protein L40	2	1
2	Thioredoxin-interacting protein	15.96	8
	Eukaryotic translation initiation factor 4B	2.25	1
	Tubulin alpha-1C chain	2	1
3	Hornerin	8	4
	Tubulin beta-3 chain	6	17
	Filaggrin	2.09	3
	RuvB-like 1	2	1

Txnip expression induced by glucose in MCF7 cells

Candidate Txnip-binding partners were identified (Table 2), however it is possible that the identified partners do not provide enough insight to understand Txnip function. To address this, we tested alternative stimulation conditions. Txnip expression is reported to be upregulated by high concentrations of glucose (10), and Txnip is assumed to play important roles in glucose metabolism (9–13). In addition, glucose suppresses AMPK, leading to the accumulation of Txnip (7). Therefore, we sought to identify Txnip-binding partners in high glucose conditions. Firstly, we checked the effect of glucose on MCF7 cells. As expected, overnight high glucose treatment upregulated Txnip in MCF7 cells (Supplementary Figure 1, lane 2). We also tested the effect of bortezomib, a proteasome inhibitor, with or without high glucose. Glucose-induced Txnip

accumulation was further augmented by bortezomib treatment (Supplementary Figure 1, lanes 6 and 8). Therefore, we used high glucose conditions for subsequent studies.

HSP90 and HSP70 proteins co-immunoprecipitated with Txnip in MCF7-Flag-HA-Txnip cells

We performed another proteomics assay, under high glucose conditions, together with SAHA and MG132**,** employing MCF7 cells stably transfected with pCMV-HA-tag or pCMV-Flag-HA-Txnip. We identified HSP90 (Heat Shock Protein 90 kDa), HSP70 (Heat Shock Protein 70 kDa), and other proteins as potential binding candidates for Txnip through mass spectrometry (Table 3 and Supplementary Table 2). To verify that these proteins bind to Txnip, we performed immunoprecipitation using anti-Flag magnetic beads to pull-down Txnip and Txnip interacting proteins. The interaction of Txnip with HSP90 (Figure 2B box) and HSP70 (Figure 2C box) was confirmed by western blotting using specific antibodies.

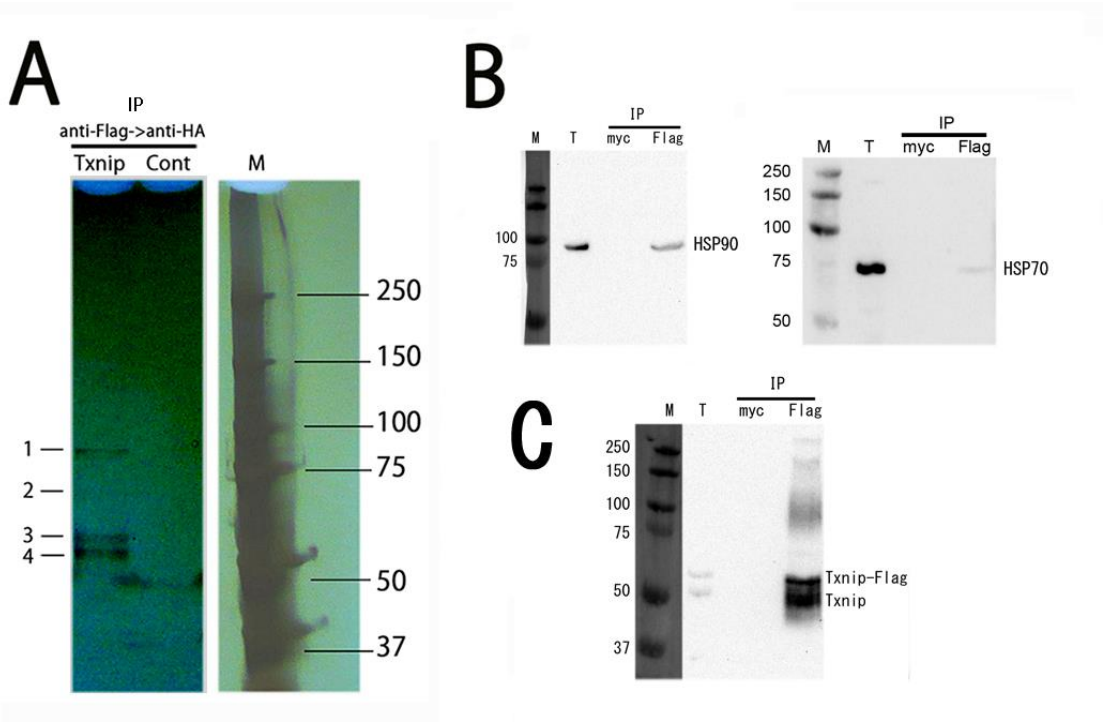

Figure 2. Identification of potential candidate proteins interacting with Txnip in MCF7 cells. (A) Silver staining of bands immunoprecipitated in tandem from MCF7-Flag-HA-Txnip (Txnip) or MCF7-Flag-HA (control) cells stimulated with 20 mM glucose overnight and with 2 μM SAHA, and 2 μM MG132. Extracts retrieved using Triton X-100 lysis buffer after discarding cytosolic fractions were used. Equal amounts of extracts were incubated with anti-Flag magnetic beads overnight at 4 °C. Beads were washed three times

with 0.05 % Tween PBS and then eluted with 3x Flag peptide (Sigma).The eluates were then incubated with anti-HA magnetic beads overnight at 4 °C. Beads were washed three times with 0.05 % Tween PBS and then eluted with HA peptide. The eluates were applied on a Precast Gel and silver stained. Indicated bands were analyzed by mass spectrometry. Candidates are shown in Table 3 and Supplementary Table 2. The image was cropped and cut for clarity. (B) Immunodetection of HSP90 and HSP70 after Flag immunoprecipitation. Extracts were immunoprecipitaed with anti-Flag or anti-Myc (control) magnetic beads. Eluates were analyzed by immunoblotting using an anti-HSP90 antibody (left) or an anti-HSP70 antibody (right). (C) Immunodetection of Txnip. The same membrane shown in Figure 2B was re-probed with an anti-Txnip antibody (Invitrogen). (IP: immunoprecipitation; WB: western blot). Images (B, C) are representative images of independently repeated experiments. Similar results are shown in Supplementary Figure 2.

Table 3. Mass spectrometry results for candidate proteins interacting with Txnip in MCF7 cells expressing either Flag-HA or Flag-HA-Txnip stimulated with high glucose, SAHA, and MG132

Band	Name	ProtScore (Unused)	Matched peptides (95%)
1	Heat shock protein 90-beta	20.99	13
	Heat shock protein 90-alpha	3.36	11
	Phosphatidylinositol 4,5-bisphosphate 3-kinase catalytic subunit alpha isoform	0.58	1
2	Heat shock 70 kDa protein 1A/1B	28	15
	Heat shock cognate 71 kDa protein	8	10
3	Thioredoxin-interacting protein	18	9
	Tubulin alpha-1C chain	6	3
	Tubulin beta-4B chain	2	1
4	Tubulin beta-4B chain	18.07	9
	Tubulin alpha-1C	16	9
	Thioredoxin-interacting protein	10.02	6
	Tubulin beta chain	4	9
	Tubulin beta-6	2	7

	Tau-tubulin kinase 1	2	1

Txnip higher-order complex localized in the nuclear fraction

To obtain the highest Txnip expression and clear negative control, we employed the Tet-on system in combination with high glucose conditions and bortezomib. Txnip expression was improved when bortezomib was used compared to MG132 (data not shown). Expression of Txnip was analyzed by treating cells with 1 µg/mL doxycycline for 48 h, followed by overnight stimulation with 20 mM glucose and 1 µM bortezomib. We observed a prominent Txnip high molecular weight native complex (Figure 3, upper left). We checked the subcellular localization of Txnip in 293 Tet-on-Txnip cells. We observed Txnip expression mainly in the nuclear hypertonic fraction and less soluble nuclear fraction which was solubilized with Triton X-100 lysis buffer from the remaining pellets after hypertonic nuclear extraction (Figure 3, B left, C, and Supplementary Figure 3).

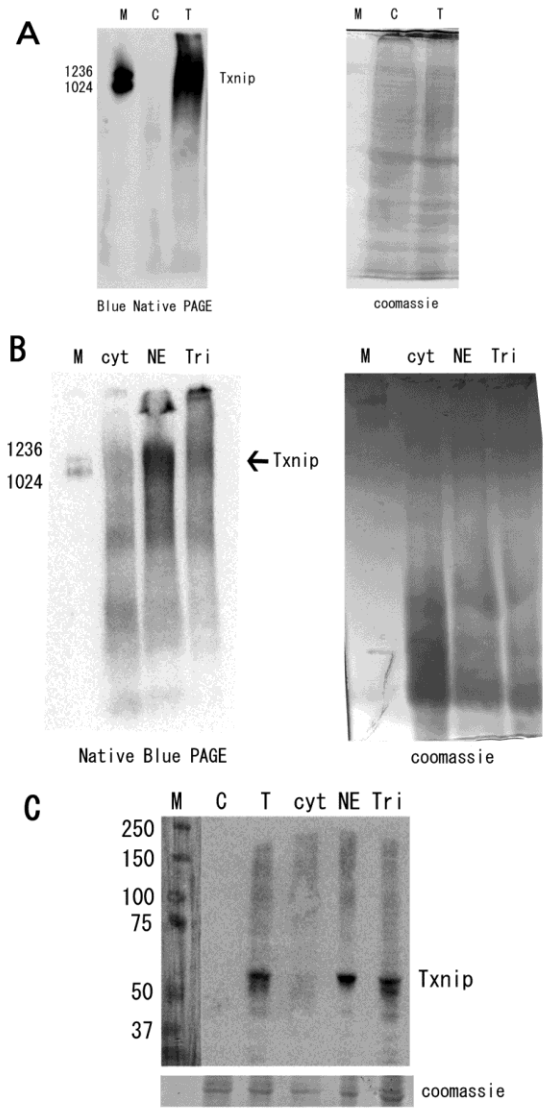

Figure 3. Txnip higher-order complex localized in the less soluble nuclear fraction. Expression of Txnip in each cellular fraction of 293 Tet-on cells transfected with a control vector or Txnip expressing vector was analyzed. Cells expressing the control vector (C) or those expressing Txnip (T) were treated with 1 μg/mL doxycycline for 48h and 20 mM glucose with 1 μM bortezomib overnight. Immunodetection of Txnip complexing at a high molecular weight (1000-1300 kDa) was then analyzed using blue native PAGE assay (A left). Coomassie Brilliant Blue staining was used as a loading control (A right). Each cellular fraction was analyzed by blue native PAGE (B left) or SDS-PAGE (C) and immunoblotting using anti-Txnip antibody (Invitrogen). Coomassie Brilliant Blue staining was used as a loading control (B right, C bottom). (M: marker; C: control; T: Txnip; cyt: cytosolic hypotonic extract; NE: nuclear hypertonic extract; Tri: Triton X-100 soluble nuclear extract from the remaining pellets after hypertonic nuclear extraction).

Txnip bound to U4/U6 small nuclear ribonucleoprotein Prp31

We showed that glucose and bortezomib treatment induced nuclear expression of Txnip and complex formation of Txnip (Figure 3). Then, we sought to identify Txnip-binding components of the high molecular weight complex in the less soluble nuclear fraction. Immunoprecipitation with anti-Flag antibody of 293 Tet-on-Txnip extracts of the less soluble nuclear fraction, concentrated by 100 kDa filtration, revealed specific Txnip candidate partner proteins, such as Prp31, 6-phosphofructo-2-kinase/fructose-2,6-bisphosphatase 3, and Filamin A, in the silver stained gel (Figure 4A, Table 4, and Supplementary Table 3). As Prp31 was one of the most abundant proteins, we focused on Prp31. Endogenous Prp31 was pulled-down from the eluate by anti-Flag antibody in 293 Tet-on cells stably transfected with the vector expressing Flag-Txnip, but not in control cells (Figure 4B). We also immunoprecipitated Prp31-myc with anti-Flag antibody in 293 Tet-on cells stably transfected with the vectors expressing Flag-Txnip and Prp31-myc, but not in cells transfected with control vector and vector expressing Prp31-myc, indicating that Txnip and Prp31 are present in the same complex (Figure 4B and C). We showed that Prp31 is co-immunoprecipitated with Txnip, but not with control (supplementary Fig.5), further suggesting the interaction between Prp31 and Txnip.

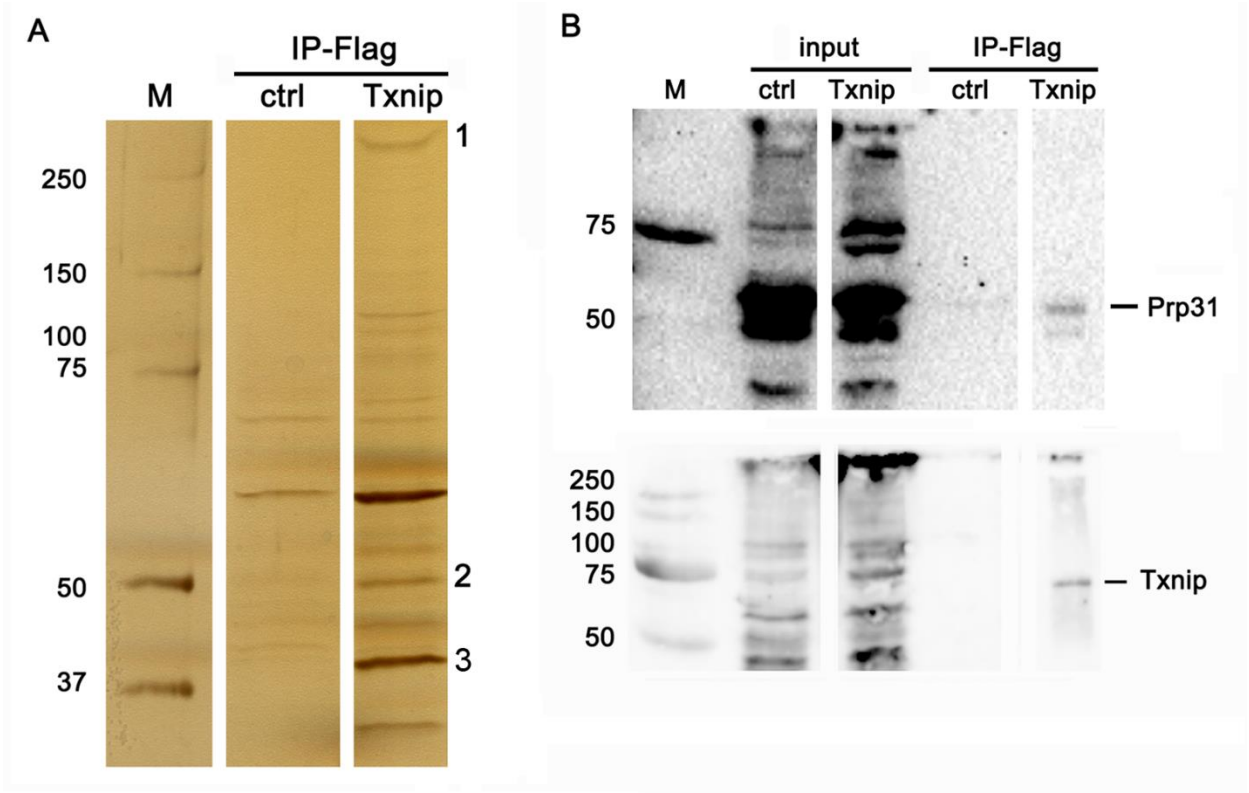

Figure 4. Identification of candidate proteins interacting with Txnip in 293 Tet-on cells transfected with Txnip, after stimulation with high glucose and bortezomib.

(A) Silver staining of Flag-immunoprecipitated proteins from 293 Tet-on cells stably transfected with either F-HA-Txnip-V5-His or control vector (ctrl) after stimulation with 1 µg/mL doxycycline (48 h) followed by overnight stimulation with 20 mM glucose with 1 µM bortezomib for 14 h. Extracts from the less soluble nuclear fraction were concentrated by 100 kDa filtration and immunoprecipitated using anti-Flag magnetic beads overnight at 4 °C. Beads were washed three times with 0.05 % Tween PBS and then eluted with a 3x Flag peptide (Sigma). The eluates were applied on a Precast Gel and silver stained. Indicated bands were analyzed by mass spectrometry. Candidate proteins are shown in Table 4 and Supplementary Table 3. (B) Detection of endogenous Prp31 protein using an anti-Prpf31 antibody in extracts immunoprecipitated using an anti-Flag antibody (upper). Re-probing of the same membrane with anti-Txnip antibody (bottom). The full-length blots are presented in Supplementary Figure 4. (M: marker; C or ctrl: control vector expressing cell; T: Txnip expressing cells).

Table 4. Mass spectrometry results for identification of candidate proteins interacting with Txnip in 293 Tet-on cells

Band	Name	ProtScore (Unused)	Matched peptides (95%)
1	Filamin A	29.79	15
	Tau-tubulin kinase 1	1.67	1
2	U4/U6 small nuclear ribonucleoprotein Prp31	23.51	13
	6-phosphofructo-2-kinase/fructose-2,6-bisphosphatase 3	12.01	6
	T-complex protein 1 subunit beta	8	4
	Tubulin alpha-1A chain	6	3
	RuvB-like 1	4	2
	RNA-binding protein 10	4	2
	Serine/threonine-protein kinase 38	2.2	2
3	Dermcidin	2	1

Txnip high molecular weight complexes were dissolved by DTT treatment

In order to analyze the constitution of the Txnip high molecular weight complex, we investigated the effects of dithiothreitol (DTT) or RNaseA on the formation of the high molecular weight complex in 293 Tet-on-Txnip cells. RNaseA treatment slightly diminished the intensity of the band (Figure 5, lane 3) while DTT treatment significantly decreased complex formation (Figure 5, lane 4). DNAase treatment did not decrease the intensity (data not shown). These results indicated that the 1000-1300 kDa Txnip complexes contain disulfide bonds and RNA.

To further analyze the RNA from the less soluble nuclear fraction, we concentrated the high molecular complexes by 100 kDa filtration of 293 Tet-on cells stably transfected with either F-HA-Txnip-V5-His or control vector after stimulation with 1 µg/mL doxycycline (24 h) followed by overnight stimulation with 100 µM 4-thiouridine (4sU), 20 mM glucose, and 1 µM bortezomib for 14 h. The RNA isolation method is described in Data in Brief. The extracted RNA was analyzed by RNA-seq (Supplementary information file 2), which showed that mRNA, lncRNA and transcripts of uncertain coding potential (TUCPs) in the complex had differential expression between Txnip and control cells. There were 1221 mRNAs differentially expressed, among which 631 were up regulated in Txnip overexpressing cells (Data in Brief, Table 1 and Figure 1) and 590 were down regulated (Data in Brief, Table 2 and Figure 1), There were 25 differentially expressed lncRNAs, among which 16 were up regulated in Txnip cells (Data in Brief Table 4 and Figure 3) and 9 were down regulated (Data in Brief, Table 5 and Figure 3). A few TUCP were also observed (Data in Brief, Table 7 and 8 and Figure 5). The gene function classification system, GO (gene ontology) enrichment of Txnip expressing and control cells showed that more than 50 percent of expressed mRNAs were involved in the biological processes (BP) of metabolism: metabolic process, cellular metabolic process, macromolecule metabolic process, etc. More than 80 percent of upregulated mRNA had the molecular function (MF) of protein binding (Data in Brief, Figure 2). In addition to that, more than 30 percent of the enriched lncRNA genes were classified as having nucleic acid binding as a molecular function (Data in Brief, Figure 4). KEGG (Kyoto Encyclopedia of Genes and Genomes) enrichment of mRNA target genes showed that they were involved in pathways in cancer, Epstein-Barr virus infection, mTOR signaling, proteoglycans in cancer, MAPK signaling pathway and influenza A (Supplementary Figure 6 and Data in Brief, Table 3). lncRNAs were involved in phagosome, Herpes simplex infection, allograft rejection, graft-versus-host disease, Type I

and II diabetes mellitus (Supplementary Figure 7 and Data in Brief Table 6). The RNAs of both control and Txnip samples showed only a small number of differential changes in alternative splicing (AS) events (Data in Brief, Table 9).

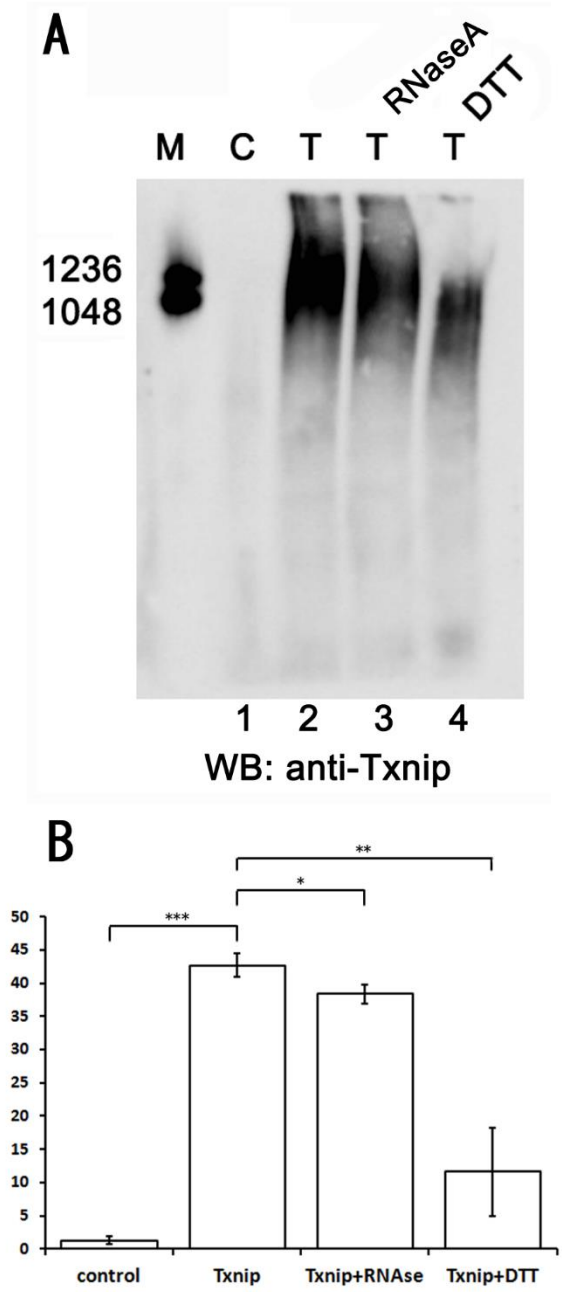

Figure 5. Txnip high molecular weight complexes were decreased by RNAse or DTT treatment. Less soluble nuclear extracts of 293 Tet-on control and Txnip cells, treated with 20 mM glucose and 10 µM bortezomib were incubated with 100 µg/ml RNaseA or 1 mM DTT and analyzed by blue native PAGE followed by incubation with anti-Txnip antibody. Results are representative f three independent experiments (M: marker; C: control; T: Txnip). (B) Quantification of the intensity of the respective bands was performed

using ImageJ and analyzed by student t-test.. Results are presented as average ±SD of three independent assays. *: P<0.05, * *: P<0.01.

Discussion

Txnip interacting partners

While Txnip is involved in numerous biological processes, the mechanisms of action of this protein have not been elucidated. In this study, we sought potential binding partners for Txnip and identified HSP90, HSP70, and Prp31 (a component of the spliceosome complex) as viable candidates.

Heat Shock Proteins (HSPs) are chaperones or guides to many key proteins that control cell growth and survival (24,25). In normal cells, most HSP proteins are ubiquitously expressed, and they usually function in conjunction with other chaperones, co-chaperones, modulators of ATPase activity, and other accessory proteins as a part of a larger complex (26). Chaperones are responsible for protein folding, quality control in the endoplasmic reticulum, and normal protein turnover (proteasomal degradation) (25). In cancer cells, HSP proteins are upregulated, indicating that they contribute to cancer progression. For example, in breast cancer, overexpression of HSP90 and HSP70 correlates with poor prognosis (27). It was reported that two HSP90 cofactors (Tah1 and Pih1) interact with the conserved AAA+-type DNA helicases Rvb1/Rvb2 (28), forming the R2TP complex (29,30). In an over-co-overexpression experiment, Txnip may directly interact with RUVBL1 (data not shown). The role of Txnip in the regulation of the R2TP complex requires further investigation.

We also detected Prp31 as a potential binding partner of Txnip. U4/U6 small nuclear ribonucleoprotein Prp31 is an important component of the spliceosome complex (31,32). Immunodepletion of this 61K-protein from HeLa nuclear extracts inhibits tri-snRNP formation and subsequent spliceosome assembly and pre-mRNA splicing (33). Txnip knockout mice exhibit significant changes in gene expression involving the PPAR pathway and insulin signaling (11,13). From this perspective, Txnip may regulate the splicing and expression of several mRNAs involved in metabolism and cancer suppression through Prp31.

Searching for "Prp31" in the Pathway Commons Protein-Protein Interactions dataset, we found that Prp31 binds to HSP90AB1, RuvB-like 1, and RuvB-like 2, further supporting our hypothesis that they could form a complex with Txnip.

Txnip redox sensitive higher-order complex

Here, we showed that Txnip forms high molecular weight complexes. Since DTT treatment significantly decreased the complex (Figure 5), a disulfide bond is required for the formation. We could speculate that thioredoxin-dependent process or oxidative stress is involved in the regulation of this complex, as Txnip acts as an endogenous negative regulator of thioredoxin (1). Further investigation is needed. RNase treatment slightly decreased the complex (Figure 5), indicating that the complex contains RNA. It has been reported that several kinds of RNAs, such as small ncRNA, miRNA, mRNA, and lncRNA act as scaffolds to nuclear proteins, RNAs and nuclear complexes (34).RNA-seq analysis showed differential expression of RNAs in the complex between Txnip overexpression and control cells (Supplementary Figures 6 and 7 and Data in Brief), indicating that Txnip influences the component of RNAs in the complex. The changes of expression were more prominent in mRNA than lncRNAs. The GO study showed that most of the upregulated mRNAs had a role in protein binding (Data in Brief, Figure 2), compatible with the formation of the ribonucleoprotein complex. Interestingly, mRNAs involved in the metabolism are enriched in association with Txnip (Data in Brief, Figure 2). This result may raise a possibility that the change of the expression or nuclear distribution of RNAs influences metabolic processes. Since more than 30 percent of the enriched lncRNA genes were classified as having nucleic acid binding as a molecular function (Data in Brief, Figure 4), the IncRNAs may have a regulatory role in nuclear events. KEGG enrichment of mRNA target genes showed that they were involved in pathways such as cancer, Epstein-Barr virus infection, mTOR signaling pathway, proteoglycans in cancer, MAPK signaling pathway and influenza A (Supplementary Figure 6 and Data in Brief, Table 3). lncRNAs were involved in phagosome, Herpes simplex infection, allograft rejection, graft-versus-host disease, Type I and II diabetes mellitus (Supplementary Figure 7 and Data in Brief, Table 6). These results may explain the pleiotropic aspects of the biological roles of Txnip in cancer suppression, diabetes and inflammation. The significance of these results should be further investigated. RNAs could serve as regulatory components of the splicing machinery along with Prp31. However, in RNA-seq results, the splicing pattern is not largely changed between Txnip overexpressing and control cells (Data in Brief, Table 9), indicating that the complex is unlikely to be involved in the splicing process.

In a yeast two-hybrid assay using Txnip (lacking the thioredoxin binding domain) as bait (Table 1), we uncovered many potential binding proteins. Interestingly, many of these are involved in DNA and RNA machinery, such as ubiquitously expressed transcript (UXT), which is a facilitator of receptor-induced

transcriptional activation; chromobox homolog 8 (CBX8), an essential component of the polycomb repressive complex essential component; integrator complex subunit 9 (INTS9), a multiprotein mediator of small nuclear RNA processing that associates with C-terminal repeat of RNA polymerase II; RuvB-like 2 (RUVBL2), a DNA helicase essential for homologous recombination; and DNA-double-strand break repair, and cisplatin resistance-associated overexpressed protein (CROP), a spliceosome protein. These results indicate that Txnip is involved in the nuclear machinery. This is most likely through the transient formation of a dynamic higher-order complex to regulate the degradation of the components upon glucose stimulation.

As Txnip participates in many processes, our hypothetical model of the mechanism of action of Txnip in the nucleus as a complex could explain its wide array of functions. The thorough elucidation of the mechanism of Txnip function will help understand its role in cancer suppression and metabolic regulation, leading to the development of new therapeutic strategies against cancer and metabolic disorders.

Acknowledgments

We thank Ms. Ryoko Otsuki, Ms. Kanari Nishioka and Ms. Sae Ashida for technical help, and Dr. Yoichi Mizutani for student guidance. This work was supported by JSPS KAKENHI Grant in Aid for Scientific Research and Innovative Areas, Scientific Research (25460386, 17K08658) from the Ministry of Education, Culture, Sports, Science and Technology (MEXT), Japan, and research grant from Kyoto University and Tenri Health Care University.

References

1. Nishiyama A, Matsui M, Iwata S, Hirota K, Masutani H, Nakamura H, et al. Identification of thioredoxin-binding protein-2/vitamin D3 up-regulated protein 1 as a negative regulator of thioredoxin function and expression. J Biol Chem. 1999;274(31):21645–50.

2. Bodnar JS, Chatterjee A, Castellani LW, Ross DA, Ohmen J, Cavalcoli J, et al. Positional cloning of the combined hyperlipidemia gene Hyplip1. Nat Genet. 2002;30(1):110–6.

3. Butler LM, Zhou X, Xu W-S, Scher HI, Rifkind RA, Marks PA, et al. The histone deacetylase inhibitor SAHA arrests cancer cell growth, up-regulates thioredoxin-binding protein-2, and down-regulates thioredoxin. Proc Natl Acad Sci. 2002;99(18):11700–5.

4. Nishinaka Y, Masutani H, Oka S, Matsuo Y, Yamaguchi Y, Nishio K, et al. Importin α1 (Rch1) mediates nuclear translocation of thioredoxin-binding protein-2 /vitamin D3 -up-regulated protein 1. J Biol Chem. 2004;279(36):37559–65.

5. Cha-Molstad H, Saxena G, Chen J, Shalev A. Glucose-stimulated expression of Txnip is mediated by carbohydrate response element-binding protein, p300, and histone H4 acetylation in pancreatic beta cells. J Biol Chem. 2009;284(25):16898–905.

6. Shaked M, Ketzinel-Gilad M, Cerasi E, Kaiser N, Leibowitz G. AMP-activated protein kinase (AMPK) mediates nutrient regulation of thioredoxin-interacting protein (TXNIP) in pancreatic beta-cells. PLoS One. 2011;6(12):e28804.

7. Wu N, Zheng B, Shaywitz A, Dagon Y, Tower C, Bellinger G, et al. AMPK-dependent degradation of TXNIP upon energy stress leads to enhanced glucose uptake via GLUT1. Mol Cell. 2013;49(6):1167–75.

8. Zhang P, Wang C, Gao K, Wang D, Mao J, An J, et al. The ubiquitin ligase itch regulates apoptosis by targeting thioredoxin-interacting protein for ubiquitin-dependent degradation. J Biol Chem. 2010;285(12):8869–79.

9. Spindel ON, World C, Berk BC. Thioredoxin interacting protein: Redox dependent and independent regulatory mechanisms. Antioxid Redox Signal. 2012;16(6):587–96.

10. Parikh H, Carlsson E, Chutkow WA, Johansson LE, Storgaard H, Poulsen P, et al. TXNIP regulates peripheral glucose metabolism in humans. PLoS Med. 2007;4(5):e158.

11. Yoshihara E, Fujimoto S, Inagaki N, Okawa K, Masaki S, Yodoi J, et al. Disruption of TBP-2 ameliorates insulin sensitivity and secretion without affecting obesity. Nat Commun. 2010;1(127):1–12.

12. Masutani H, Yoshihara E, Masaki S, Chen Z, Yodoi J. Thioredoxin binding protein (TBP)-2/Txnip and α-arrestin proteins in cancer and diabetes mellitus. J Clin Biochem Nutr. 2012;50(1):23–34.

13. Oka SI, Yoshihara E, Bizen-Abe A, Liu W, Watanabe M, Yodoi J, et al. Thioredoxin binding protein-2/thioredoxin-interacting protein is a critical regulator of insulin secretion and peroxisome proliferator-activated receptor function. Endocrinology. 2009;150(3):1225–34.

14. Nishinaka Y, Nishiyama A, Masutani H, Oka SI, Ahsan KM, Nakayama Y, et al. Loss of thioredoxin-binding protein-2/vitamin D3 up-regulated protein 1 in human T-cell leukemia virus type I-dependent T-cell transformation: Implications for adult T-cell leukemia leukemogenesis. Cancer Res. 2004;64(4):1287–92.

15. Ahsan MK, Masutani H, Yamaguchi Y, Kim Y-C, Nosaka K, Matsuoka M, et al. Loss of interleukin-2-dependency in HTLV-I-infected T cells on gene silencing of thioredoxin-binding protein-2. Oncogene. 2006;25:2181–91.

16. Kwon H-J, Won Y-S, Suh H-W, Jeon J-H, Shao Y, Yoon S-R, et al. Vitamin D3 upregulated protein 1 suppresses TNF-α-induced NF-κB activation in hepatocarcinogenesis. J Immunol. 2010;185:3980–9.

17. Ikarashi M, Takahashi Y, Ishii Y, Nagata T, Asai S, Ishikawa K. Vitamin D3 up-regulated protein 1 (VDUPI) expression in gastrointestinal cancer and its relation to stage of disease. Anticancer Res. 2002;22(6C):4045–8.

18. Nishizawa K, Nishiyama H, Matsui Y, Kobayashi T, Saito R, Kotani H, et al. Thioredoxin-interacting protein suppresses bladder carcinogenesis. Carcinogenesis. 2011;32(10):1459–66.

19. Masaki S, Masutani H, Yoshihara E, Yodoi J. Deficiency of thioredoxin binding protein-2 (TBP-2) enhances TGF-β signaling and promotes epithelial to mesenchymal transition. PLoS One. 2012;7(6):e39900.

20. Ago T, Liu T, Zhai P, Chen W, Li H, Molkentin JD, et al. A redox-dependent pathway for regulating class II HDACs and cardiac hypertrophy. Cell. 2008;133:978–93.

21. Jeon JH, Lee KN, Hwang CY, Kwon KS, You KH, Choi I. Tumor suppressor VDUP1 increases p27kip1 stability by inhibiting JAB1. Cancer Res. 2005;65(11):4485–9.

22. Schroder K, Zhou R, Tschopp J. The NLRP3 inflammasome: A sensor for metabolic danger? Science. 2010 Jan 15;327(5963):296–300.

23. Lee S, Min Kim S, Dotimas J, Li L, Feener EP, Baldus S, et al. Thioredoxin-interacting protein regulates protein disulfide isomerases and endoplasmic reticulum stress. EMBO Mol Med. 2014;6(6):732–43.

24. Whitesell L, Lindquist SL. HSP90 and the chaperoning of cancer. Nat Rev Cancer. 2005 ;5(10):761–72.

25. Araki K, Nagata K. Protein folding and quality control in the ER. Cold Spring Harb Perspect Biol. 2011;3(11):a007526.

26. Wegele H, Müller L, Buchner J. Hsp70 and Hsp90--a relay team for protein folding. Rev Physiol Biochem Pharmacol. vol 151. 2004;151:1–44.

27. Yano M, Naito Z, Tanaka S, Asano G. Expression and roles of heat shock proteins in human breast cancer. Jpn J Cancer Res. 1996;87(9):908–15.

28. Zhao R, Davey M, Hsu YC, Kaplanek P, Tong A, Parsons AB, et al. Navigating the chaperone network: An integrative map of physical and genetic interactions mediated by the hsp90 chaperone. Cell. 2005;120(5):715–27.

29. Kakihara Y, Houry WA. The R2TP complex: Discovery and functions. Biochim Biophys Acta - Mol Cell Res. 2012;1823(1):101–7.

30. Bizarro J, Dodré M, Huttin A, Charpentier B, Schlotter F, Branlant C, et al. NUFIP and the HSP90/R2TP chaperone bind the SMN complex and facilitate assembly of U4-specific proteins. Nucleic Acids Res. 2015;43(18):8973–89.

31. Weidenhammer EM, Singh M, Ruiz-Noriega M, Woolford JL. The *PRP31* gene encodes a novel protein required for pre-mRNA splicing in *Saccharomyces cerevisiae*. Nucleic Acids Res. 1996;24(6):1164–70.

32. Weidenhammer EM, Ruiz-Noriega M, Woolford JL. Prp31p promotes the association of the U4/U6 U5 Tri-snRNP with prespliceosomes to form spliceosomes in *Saccharomyces cerevisiae*. Mol Cell Biol. 1997;17(7):3580–8.

33. Makarova O V., Makarov EM, Liu S, Vornlocher H-P, Lurmann R. Protein 61K, encoded by a gene (PRPF31) linked to autosomal dominant retinitis pigmentosa, is required for U4.U6 U5 tri-snRNP formation and pre-mRNA splicing. EMBO J. 2002;21(5):1148–57.

34. Yoon JH, Abdelmohsen K, Gorospe M. Functional interactions among microRNAs and long noncoding RNAs. Semin Cell Dev Biol. 2014;34:9–14.

Supporting information

Supplementary Figure 1. Accumulation of Txnip expression after high glucose treatment. MCF7 cells were treated with 5 mM or 20 mM glucose overnight with 10 μM bortezomib for the indicated times. Total cell extracts were analyzed by western blotting using an anti-Txnip antibody (upper) or an anti-actin antibody (lower).

Supplementary Figure 2. Identification of potential candidate proteins interacting with Txnip in MCF7 cells.

(A) Immunodetecion of HSP90. MCF7-Flag-HA-Txnip (Txnip) or MCF7-Flag-HA (control) cells were stimulated with 20 mM glucose overnight and with 2 µM SAHA, and 2 µM MG132 for 6h. Extracts were retrieved using Triton X-100 lysis buffer after discarding cytosolic fractions. Equal amounts of extracts were incubated with anti-Flag magnetic beads overnight at 4 °C. Beads were washed three times with 0.05 % Tween-PBS and then eluted with 3x Flag peptide (Sigma).The eluates were then incubated with anti-HA magnetic beads overnight at 4 °C. Beads were washed three times with 0.05 % Tween-PBS and then eluted with HA peptide. Eluates were analyzed by Western blotting.

(B) Immunodetection of HSP70. The same membrane shown in A was re-probed with an anti-HSP70 antibody. (IP: immunoprecipitation; WB: western blot).

Supplementary Figure 3. Expression of RNA polymerase II in each fraction. The same membrane of Figure 3B was reblotted with an anti-RNA polymerase II antibody (Active Motif).

Supplementary Figure 4. Complete images of those shown in Figure 4. (A) Complete silver stained gel image for Figure 4A. Extracts from the less soluble nuclear fraction of 293 Tet-on cells stably transfected with either F-HA-Txnip-V5-His or control vector, after stimulation with 1 µg/mL doxycycline (48 h) followed by overnight stimulation with 20 mM glucose with 1 µM bortezomib for 14 h, were concentrated by 100 kDa filtration. The extracts were immunoprecipitated using an anti-Flag magnetic beads overnight at 4 °C. The beads were washed three times with 0.05 % Tween-PBS and then eluted with 3x Flag peptide (Sigma). The eluates were applied on a Precast Gel and silver stained. (B) Full-length western blot images for Figure 4B. Detection of endogenous Prp31 protein using an anti-Prp31 antibody in extracts immunoprecipitated using anti-Flag magnetic beads (upper). Re-probing of the same membrane with an anti-Txnip antibody (bottom). (M: marker; C or ctrl: control vector expressing cells; Txnip: Txnip expressing cells).

Supplementary Figure 5. Interaction between Txnip and Prp31. Tet on 293 cells stably transfected with F-HA-Txnip-V5-His and Myc-Prp31 were treated with 1 µg/mL doxycycline (24 h) followed by overnight stimulation with 20 mM glucose with 1 µM bortezomib for 14 h. Extracts from the less soluble nuclear fraction were treated with DNase and immunoprecipitated using anti-Flag magnetic beads or control magnetic beads (Dynabeeds M-280 anti-mouse IgG; Invitrogen) overnight at 4 °C. Beads were washed three times with

0.05 % Tween-PBS and then eluted with a 3x Flag peptide (Sigma). The eluates were analyzed by western blotting using anti-Txnip (ab18865, Abcam) (left) or anti-Prp31 antibody (right), respectively (M: marker; TP: cells expressing Flag-Txnip and Prp31-myc). The figure shown is a representative image of two independent experiments. pFN21A-Prp31-Halotag was bought from Promega (Madison, WI). Using the vector as a template, Prp31 gene sequence was amplified by PCR with primers 5′-GGATCCATGTCTCTGGCAGATGAGCTCTTA-3′ and 5′-CCGCGGTCAGGTGGACATAAGGCCACTCTT-3′, containing BamHI and SacII cloning sites. After verification of the sequence, the amplified products were inserted into pCR-Blunt II-TOPO® (Invitrogen, Carlsbad, CA) and then the BamHI-EcoRI cloning site was inserted into pCMV-Tag3B, resulting in pCMV-Tag3B-Prp31 vector.

Supplementary Figure 6. Scatter plot of KEGG enrichment of mRNA target genes comparing Txnip overexpressing and control cells. RNAs from the complex of Txnip and control cells were analyzed. The number of enriched genes on each pathway is shown. Rich factor is the ratio between enriched candidate genes number and total annotated gene number in individual pathway. The higher the Rich factor is the heavier of the enrichment will be. qvalue is multiple test adjusted pvalue. qvalue should be [0, 1]. The closer to 0, the more significantly enriched. The size and color of point represent the number of differential genes in the pathway and the range of different Q value, respectively.

Supplementary Figure 7. Scatter plot of KEGG enrichment of lncRNA target genes comparing Txnip overexpressing and control cells. RNAs from the complex of Txnip and control cells were analyzed. The number of enriched genes on each pathway is shown. Rich factor is the ratio between enriched candidate genes number and total annotated gene number in individual pathway. The higher the Rich factor is the heavier of the enrichment will be. qvalue is multiple test adjusted pvalue. qvalue should be [0, 1]. The closer to 0, the more significantly enriched. The size and color of point represent the number of differential genes in the pathway and the range of different Q value, respectively.

Supplementary Table 1. Mass spectrometry results for candidate proteins interacting with Txnip in MCF7 cells stimulated with SAHA and MG132

Supplementary Table 2. Mass spectrometry results for candidate proteins interacting with Txnip in MCF7 cells expressing either Flag-HA or Flag-HA-Txnip stimulated with high glucose, SAHA, and MG132

Supplementary Table 3. Mass spectrometry results for identification of candidate proteins interacting with Txnip in 293 Tet-on cells

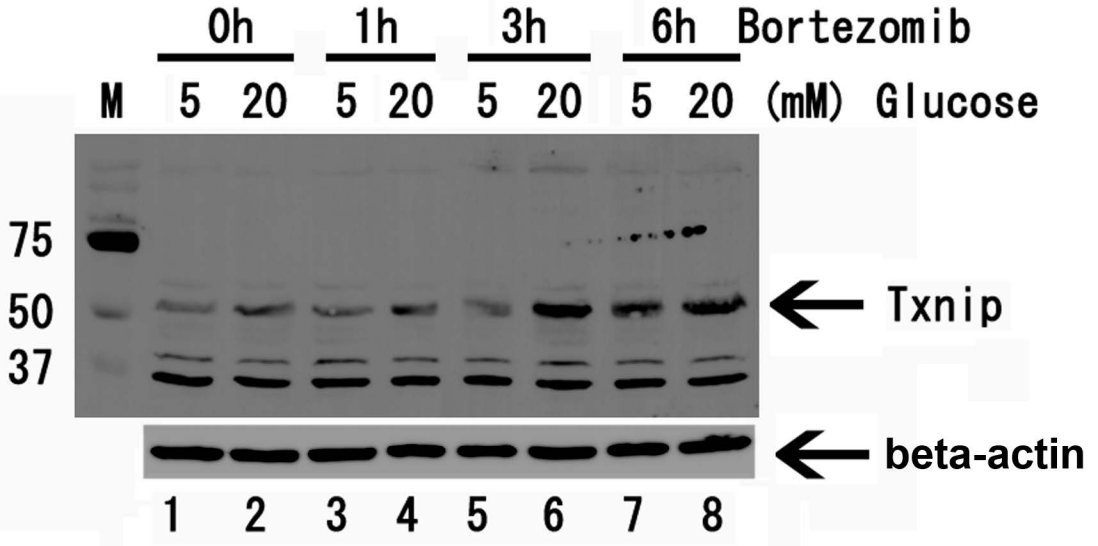
0h
1h
3h
6h
Bortezomib
M
5
20
5
20
5
20
5
20
(mM) Glucose
75
50
37
Txnip
beta-actin
1
2
3
4
5
6
7
8

A

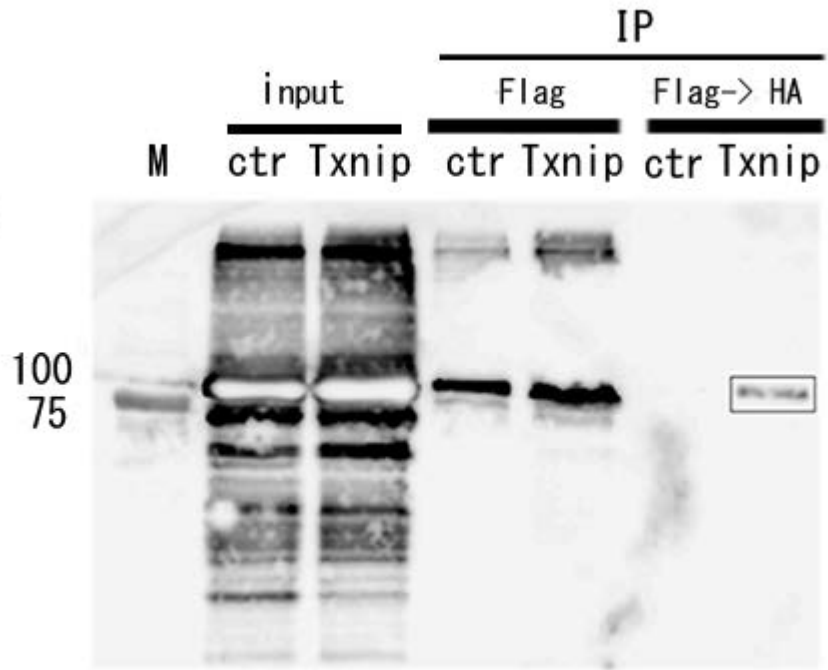

WB: anti-HSP90

B

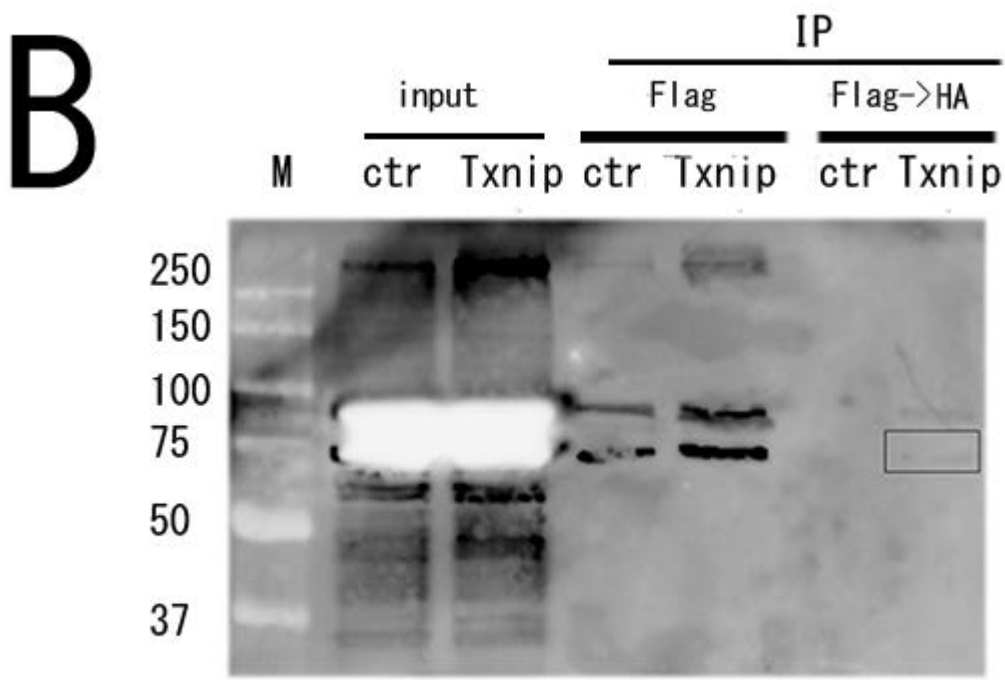

WB: anti-HSP70

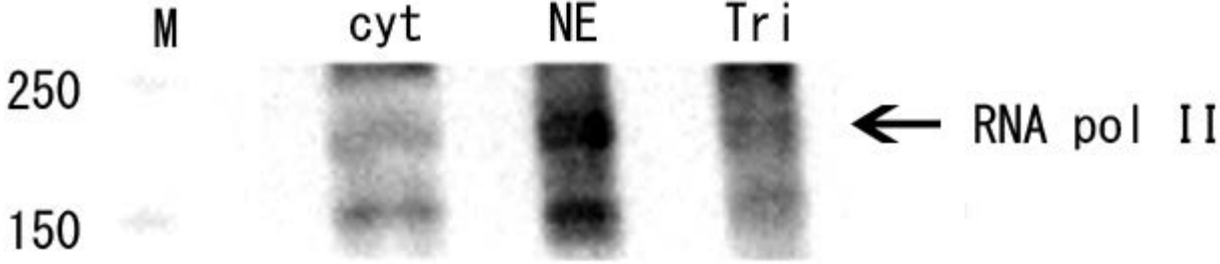
M
cyt
NE
Tri
250
150
RNA pol II

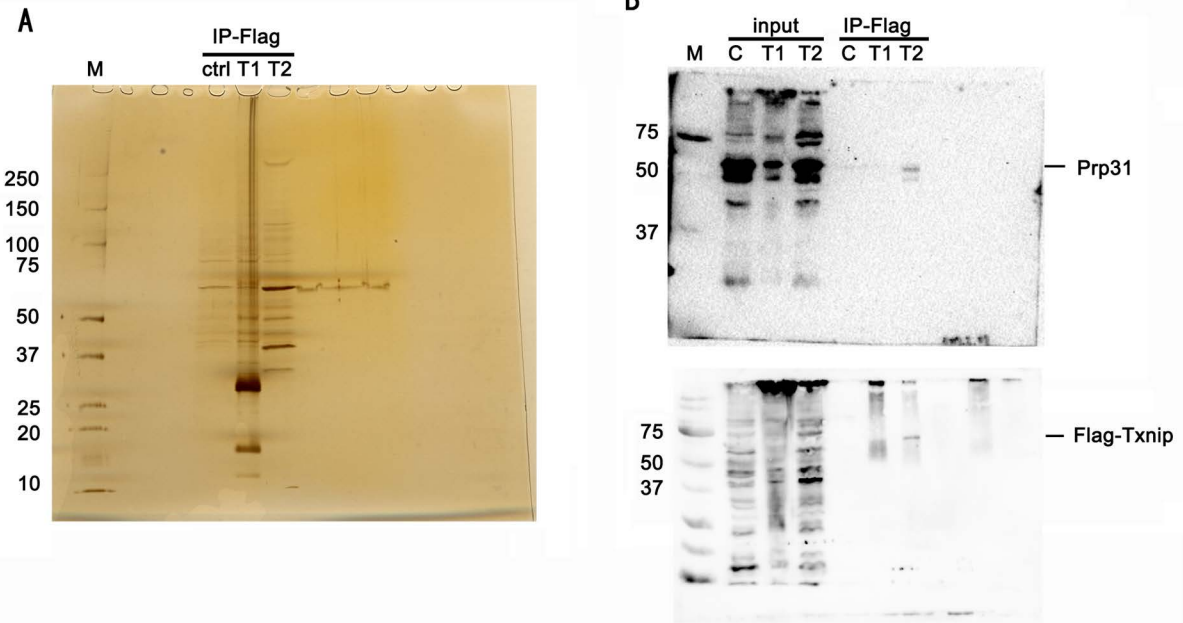
A
IP-Flag
M
ctrl T1 T2
250
150
100
75
50
37
25
20
10
B
input
IP-Flag
M
C T1 T2
C T1 T2
75
50
37
Prp31
75
50
37
Flag-Txnip

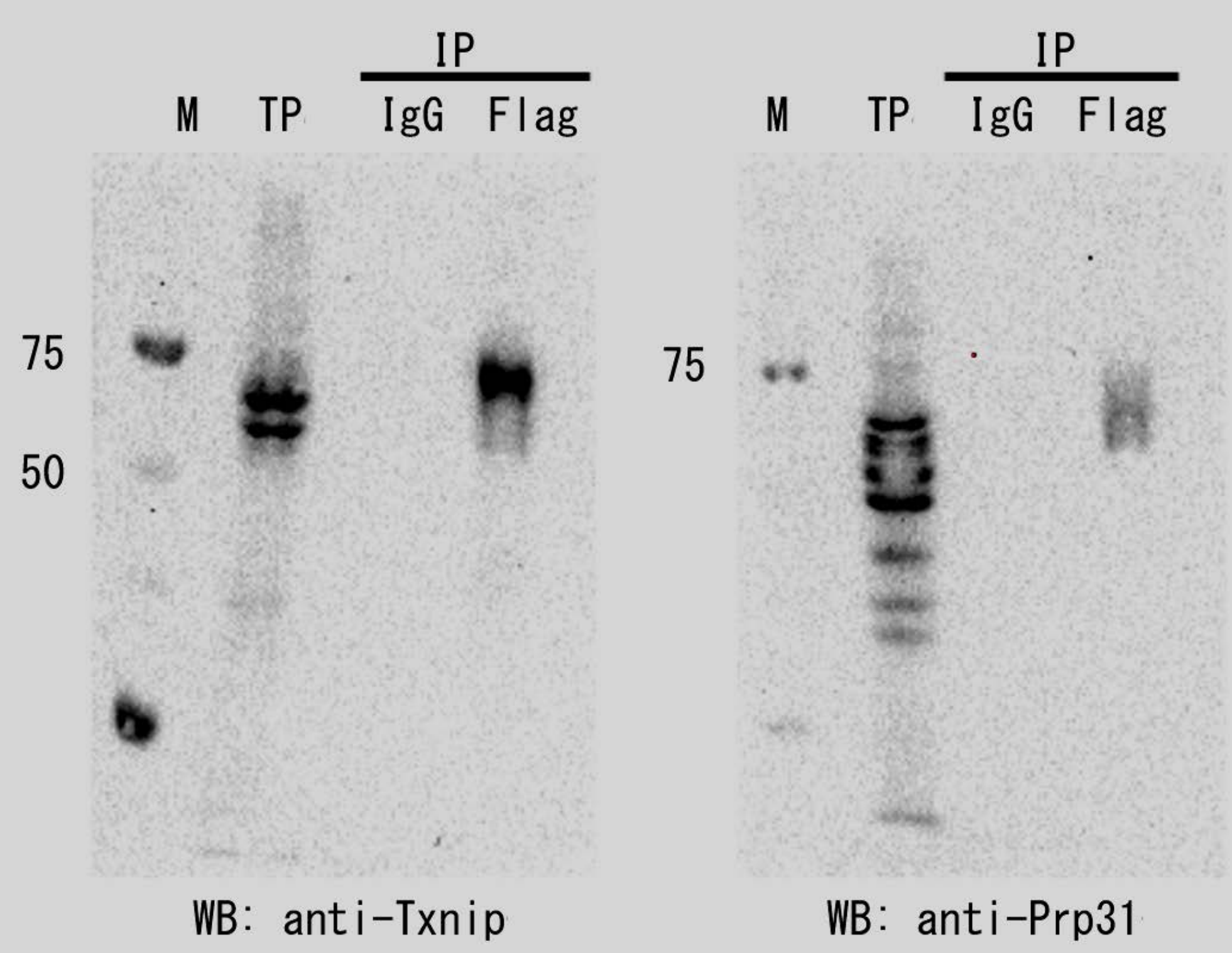
IP
M
TP
IgG
Flag
75
50
WB: anti-Txnip
IP
M
TP
IgG
Flag
75
WB: anti-Prp31

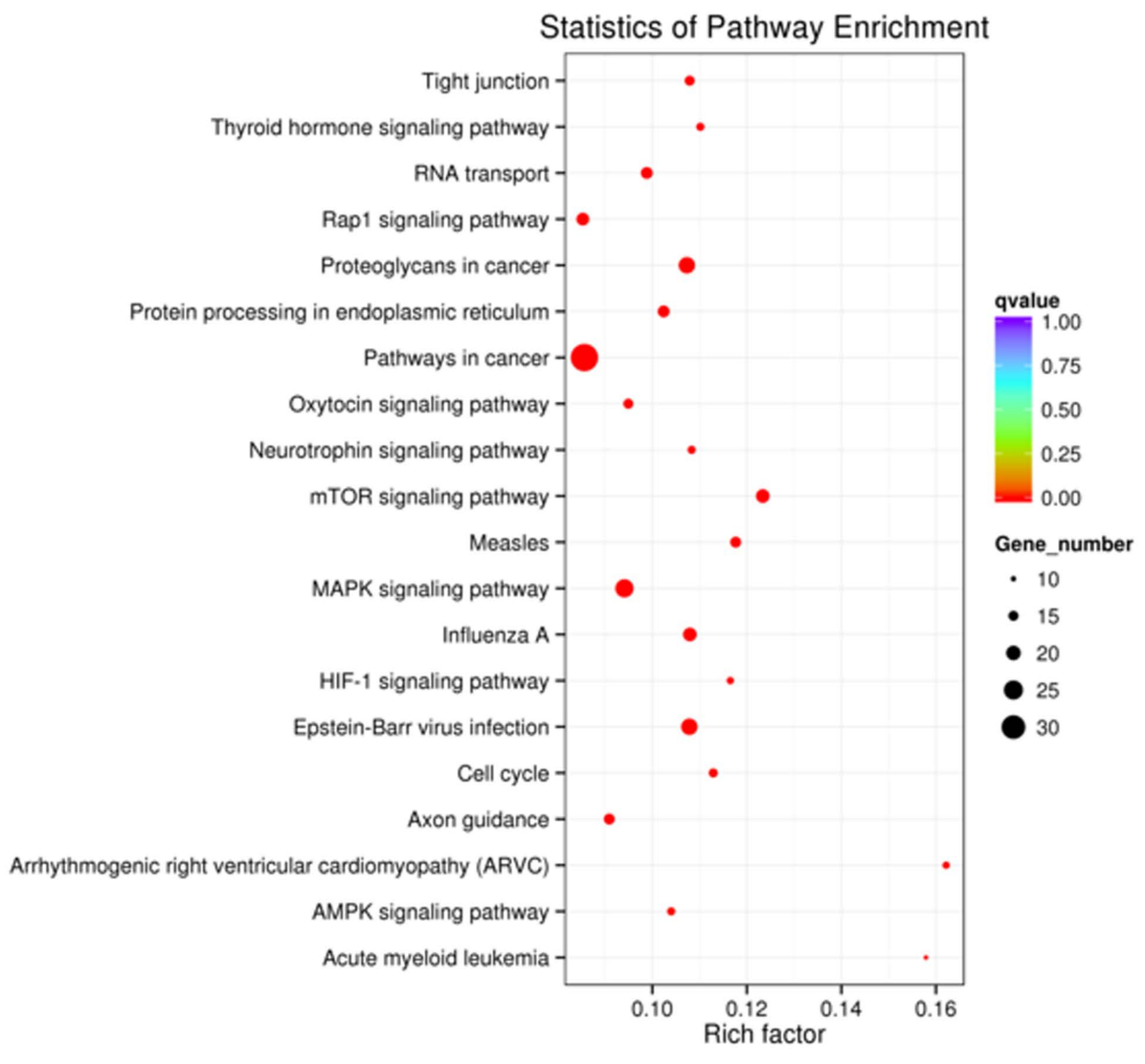
Statistics of Pathway Enrichment
Tight junction
Thyroid hormone signaling pathway
RNA transport
Rap1 signaling pathway
Proteoglycans in cancer
Protein processing in endoplasmic reticulum
Pathways in cancer
Oxytocin signaling pathway
Neurotrophin signaling pathway
mTOR signaling pathway
Measles
MAPK signaling pathway
Influenza A
HIF-1 signaling pathway
Epstein-Barr virus infection
Cell cycle
Axon guidance
Arrhythmogenic right ventricular cardiomyopathy (ARVC)
AMPK signaling pathway
Acute myeloid leukemia
0.10
0.12
0.14
0.16
Rich factor
qvalue
1.00
0.75
0.50
0.25
0.00
Gene_number
10
15
20
25
30

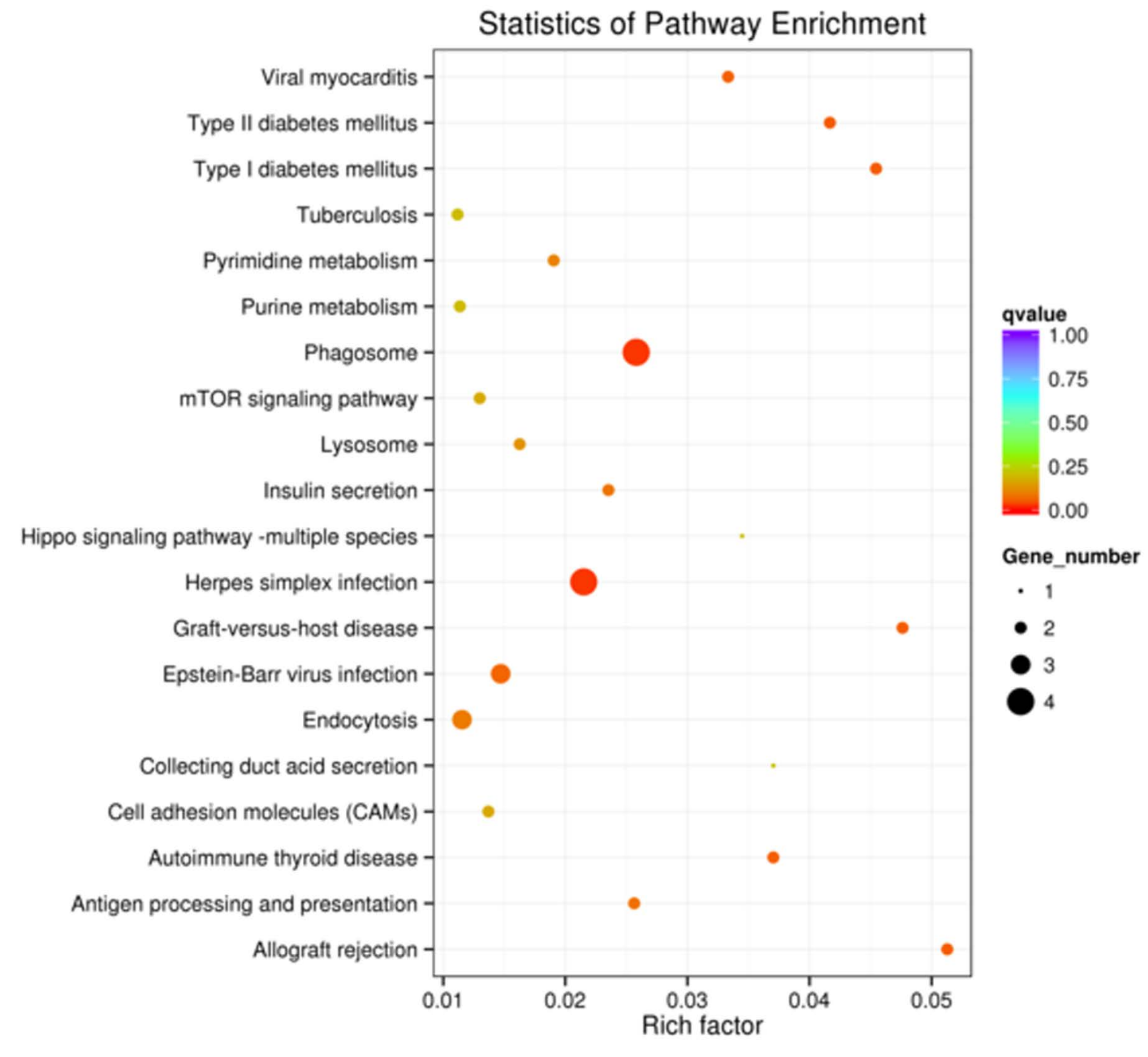
Statistics of Pathway Enrichment
Viral myocarditis
Type II diabetes mellitus
Type I diabetes mellitus
Tuberculosis
Pyrimidine metabolism
Purine metabolism
Phagosome
mTOR signaling pathway
Lysosome
Insulin secretion
Hippo signaling pathway -multiple species
Herpes simplex infection
Graft-versus-host disease
Epstein-Barr virus infection
Endocytosis
Collecting duct acid secretion
Cell adhesion molecules (CAMs)
Autoimmune thyroid disease
Antigen processing and presentation
Allograft rejection
0.01
0.02
0.03
0.04
0.05
Rich factor
qvalue
1.00
0.75
0.50
0.25
0.00
Gene_number
1
2
3
4

Supplementary Table 1

Mass spectrometry results for candidate proteins interacting with Txnip in MCF7 cells expressing either Flag-HA or Flag-HA-Txnip stimulated with SAHA and MG132

Band 1

ProtScore (Unused)	Peptides (95%)	Accession #	Name
56.18	39	sp|P23588|IF4B_HUMAN	Eukaryotic translation initiation factor 4B
2	1	sp|Q86YZ3|HORN_HUMAN	Hornerin
2	1	sp|Q12912|LRMP_HUMAN	Lymphoid-restricted membrane protein
2	1	sp|P62987|RL40_HUMAN	Ubiquitin-60S ribosomal protein L40

Band 1 (control)

ProtScore (Unused)	Peptides (95%)	Accession #	Name
24	13	sp|P23588|IF4B_HUMAN	Eukaryotic translation initiation factor 4B

Band 2

ProtScore (Unused)	Peptides (95%)	Accession #	Name
15.96	8	sp|Q9H3M7|TXNIP_HUMAN	Thioredoxin-interacting protein
11.66	8	sp|Q86YZ3|HORN_HUMAN	Hornerin
2.25	1	sp|P23588|IF4B_HUMAN	Eukaryotic translation initiation factor 4B
2	1	sp|P14923|PLAK_HUMAN	Junction plakoglobin
2	1	sp|Q9BQE3|TBA1C_HUMAN	Tubulin alpha-1C chain
2	1	sp|Q08554|DSC1_HUMAN	Desmocollin-1

Band 2 (control)

ProtScore (Unused)	Peptides (95%)	Accession #	Name
14	9	sp|Q86YZ3|HORN_HUMAN	Hornerin
7.54	4	sp|P15924|DESP_HUMAN	Desmoplakin
4	2	sp|Q01469|FABP5_HUMAN	Fatty acid-binding protein, epidermal
4	2	sp|P14923|PLAK_HUMAN	Junction plakoglobin
2	1	sp|Q5D862|FILA2_HUMAN	Filaggrin-2
2	1	sp|Q96P63|SPB12_HUMAN	Serpin B12
2	1	sp|P81605|DCD_HUMAN	Dermcidin

Band 3

ProtScore (Unused)	Peptides (95%)	Accession #	Name
30.01	22	sp|P68371|TBB4B_HUMAN	Tubulin beta-4B chain
21.89	13	sp|Q9BQE3|TBA1C_HUMAN	Tubulin alpha-1C chain
8	4	sp|Q86YZ3|HORN_HUMAN	Hornerin
6	17	sp|Q13509|TBB3_HUMAN	Tubulin beta-3 chain
2.09	3	sp|P20930|FILA_HUMAN	Filaggrin
2	22	sp|P07437|TBB5_HUMAN	Tubulin beta chain
2	1	sp|P23588|IF4B_HUMAN	Eukaryotic translation initiation factor 4B
2	1	sp|Q9Y265|RUVB1_HUMAN	RuvB-like 1

Band 3 (control)

ProtScore (Unused)	Peptides (95%)	Accession #	Name
9.7	5	sp|P68371|TBB4B_HUMAN	Tubulin beta-4B chain
6	3	sp|Q9BQE3|TBA1C_HUMAN	Tubulin alpha-1C chain
4	2	sp|P23588|IF4B_HUMAN	Eukaryotic translation initiation factor 4B
2	5	sp|P07437|TBB5_HUMAN	Tubulin beta chain

Supplementary Table 2

Mass spectrometry results for candidate proteins interacting with Txnip in MCF7 cells expressing either Flag-HA or Flag-HA-Txnip stimulated with high glucose, SAHA, and MG132

Band 1

ProtScore (Unused)	Peptides (95%)	Accession #	Name
20.99	13	sp|P08238|HS90B_HUMAN	Heat shock protein HSP 90-beta
3.36	11	sp|P07900|HS90A_HUMAN	Heat shock protein HSP 90-alpha
0.58	1	sp|P42336|PK3CA_HUMAN	Phosphatidylinositol 4,5-bisphosphate 3-kinase catalytic subunit alpha isoform

Band 1(control)

ProtScore (Unused)	Peptides (95%)	Accession #	Name
2	1	sp|Q12931|TRAP1_HUMAN	Heat shock protein 75 kDa, mitochondrial

Band 2

ProtScore (Unused)	Peptides (95%)	Accession #	Name
28	15	sp|P08107|HSP71_HUMAN	Heat shock 70 kDa protein 1A/1B
8	10	sp|P11142|HSP7C_HUMAN	Heat shock cognate 71 kDa protein
2	1	sp|P14923|PLAK_HUMAN	Junction plakoglobin

Band 2 (control)

ProtScore (Unused)	Peptides (95%)	Accession #	Name
13.76	7	sp|P15924|DESP_HUMAN	Desmoplakin
6	3	sp|P81605|DCD_HUMAN	Dermcidin
4	2	sp|Q5D862|FILA2_HUMAN	Filaggrin-2
4	2	sp|Q86YZ3|HORN_HUMAN	Hornerin
2	1	sp|P14923|PLAK_HUMAN	Junction plakoglobin
2	1	sp|Q08554|DSC1_HUMAN	Desmocollin-1
1.06	1	sp|Q5T750|XP32_HUMAN	Skin-specific protein 32

Band 3

ProtScore (Unused)	Peptides (95%)	Accession #	Name
18	9	sp|Q9H3M7|TXNIP_HUMAN	Thioredoxin-interacting protein
6	3	sp|Q9BQE3|TBA1C_HUMAN	Tubulin alpha-1C chain
2	1	sp|P68371|TBB4B_HUMAN	Tubulin beta-4B chain

Band 3 (control)

ProtScore (Unused)	Peptides (95%)	Accession #	Name

Band 4

ProtScore (Unused)	Peptides (95%)	Accession #	Name
18.07	9	sp|P68371|TBB4B_HUMAN	Tubulin beta-4B chain
16	9	sp|Q9BQE3|TBA1C_HUMAN	Tubulin alpha-1C chain
10.02	6	sp|Q9H3M7|TXNIP_HUMAN	Thioredoxin-interacting protein
4	9	sp|P07437|TBB5_HUMAN	Tubulin beta chain
2	7	sp|Q9BUF5|TBB6_HUMAN	Tubulin beta-6 chain
2	1	sp|Q5TCY1|TTBK1_HUMAN	Tau-tubulin kinase 1

Band 4 (control)

ProtScore (Unused)	Peptides (95%)	Accession #	Name
6	4	sp|Q86YZ3|HORN_HUMAN	Hornerin
5.16	3	sp|P15924|DESP_HUMAN	Desmoplakin
2	1	sp|Q96P63|SPB12_HUMAN	Serpin B12
0.23	1	sp|P14923|PLAK_HUMAN	Junction plakoglobin

Supplementary Table 3

Mass spectrometry results for identification of candidate proteins interacting with Txnip in 293 Tet-on cells expressing either control or Flag-HA-Txnip-V5-His stimulated with high glucose and bortezomib

Band 1

ProtScore (Unused)	Peptides (95%)	Accession #			Name
29.79	15	sp	P21333	FLNA_HUMAN	Filamin-A
1.67	1	sp	Q5TCY1	TTBK1_HUMAN	Tau-tubulin kinase 1

Band 1 (control)

ProtScore (Unused)	Peptides (95%)	Accession #	Name

Band 2

ProtScore (Unused)	Peptides (95%)	Accession #			Name
23.51	13	sp	Q8WWY3	PRP31_HUMAN	U4/U6 small nuclear ribonucleoprotein Prp31
20	10	sp	P07437	TBB5_HUMAN	Tubulin beta chain
12.01	6	sp	Q16875	F263_HUMAN	6-phosphofructo-2-kinase/fructose-2,6-bisphosphatase 3
8	4	sp	P78371	TCPB_HUMAN	T-complex protein 1 subunit beta
6	3	sp	Q71U36	TBA1A_HUMAN	Tubulin alpha-1A chain
4	2	sp	P23588	IF4B_HUMAN	Eukaryotic translation initiation factor 4B
4	2	sp	Q9Y265	RUVB1_HUMAN	RuvB-like 1
4	2	sp	P98175	RBM10_HUMAN	RNA-binding protein 10
2.2	2	sp	Q15208	STK38_HUMAN	Serine/threonine-protein kinase 38

Band 2 (control)

ProtScore (Unused)	Peptides (95%)	Accession #			Name
10	5	sp	P07437	TBB5_HUMAN	Tubulin beta chain
6	3	sp	P23588	IF4B_HUMAN	Eukaryotic translation initiation factor 4B
6	3	sp	Q9BQE3	TBA1C_HUMAN	Tubulin alpha-1C chain
2	2	sp	Q12912	LRMP_HUMAN	Lymphoid-restricted membrane protein

Band 3

ProtScore (Unused)	Peptides (95%)	Accession #			Name
14	10	sp	Q9BQA1	MEP50_HUMAN	Methylosome protein 50
9.63	5	sp	P23588	IF4B_HUMAN	Eukaryotic translation initiation factor 4B
2	1	sp	P81605	DCD_HUMAN	Dermcidin

Band 3 (control)

ProtScore (Unused)	Peptides (95%)	Accession #			Name
17.91	9	sp	P23588	IF4B_HUMAN	Eukaryotic translation initiation factor 4B
3.7	2	sp	P04075	ALDOA_HUMAN	Fructose-bisphosphate aldolase A
2	1	sp	P98175	RBM10_HUMAN	RNA-binding protein 10
0.92	1	sp	Q9BQA1	MEP50_HUMAN	Methylosome protein 50